Journal of Luminescence 132 (2012) 3072–3076

Contents lists available at SciVerse ScienceDirect

Journal of Luminescence

journal homepage: www.elsevier.com/locate/jlumin

A potential red emitting $K_4Ca(PO_4)_2$: Eu^{3+} phosphor for white light emitting diodes

G.R. Dillip [a], S.J. Dhoble [b], L. Manoj [c], C. Madhukar Reddy [a], B. Deva Prasad Raju [a,d,*]

[a] Department of Physics, Sri Venkateswara University, Tirupati 517502, India
[b] Department of Physics, RTM Nagpur University, Nagpur 440033, India
[c] Centre for Nanoscience and Nanotechnology, Sathyabama University, Chennai 600119, India
[d] Department of Future Studies, Sri Venkateswara University, Tirupati 517502, India

ARTICLE INFO

Article history:
Received 25 February 2012
Received in revised form
7 May 2012
Accepted 18 June 2012
Available online 2 July 2012

Keywords:
Strong red-emission
SEM
Decay curves
DSC
LED phosphor

ABSTRACT

Europium (III) ions doped red phosphors $K_4Ca(PO_4)_2$ were prepared first time by high temperature solid state reaction method. The prepared phosphors structure was examined by X-ray diffraction (XRD), Fourier transform infrared (FTIR) spectroscopy, scanning electron microscopy (SEM), and energy dispersive spectroscopy (EDS) analyses. The thermal properties of the synthesized phosphor were investigated by differential scanning calorimetry (DSC) analysis. Photoluminescence (PL) spectra of $K_4Ca(PO_4)_2$:Eu^{3+} phosphors have shown strong red emission at 618 nm ($^5D_0 \rightarrow {}^7F_2$) with near UV an excitation wavelength of λ_{exc}=394 nm ($^7F_0 \rightarrow {}^5L_6$). In addition, the decay curves and CIE color coordinate measurements are also carried out. Hence, emission and excitation characterization of synthesized phosphors shows that the phosphors may be a promising red component for the application in the white light emitting diodes (WLEDs).

1. Introduction

Now-a-days the sustainable development of the society is based on the energy crises and environmental pollution. To overcome the present problems the new clean energy source and energy saving devices are required. The light emitting diodes (LEDs) are an ideal energy saving and environmentally friendly devices. The various inorganic phosphor materials activated with rare earth ions attracted considerable attention owing to their wide and potential applications in the emerging field of display and luminescent devices. These include optical filters, solid state lasers (SSL), fluorescent lamps, cathode ray tubes, field emission displays, plasma displays, and white light emitting diodes (WLEDs) [1–4]. White LEDs hold much attention to be a next-generation light source due to their high efficiency, low power consumption, long lifetime, fast response, energy saving and environment friendliness, etc. The current commercial way to generate white light is to combine blue chips with yellow phosphors (YAG:Ce^{3+}) [5,6]. Although, this kind of white light blending method has been used for many years, some serious problems still exist, such as due to the scarcity of the red emission from YAG:Ce^{3+}, the obtained white light has low color rendering index (CRI) ($Ra < 80$), high color temperature (usually above 5000 K), and narrow visible range [7,8]. To avoid these deficiencies, another strategy to produce white light is by combining near UV LED with tricolors (red, green and blue) (RGB) phosphors. NUV phosphor converted LEDs are expected to have many potential applications, due to their excellent color rendering index, high color tolerance and high conversion efficiency into visible light [9,10]. Regrettably, currently used red phosphors Y_2O_2S:Eu^{3+} and $Ca_{1-x}Sr_xS$:Eu^{2+} for WLEDs do not have enough absorption in the near-UV region and are environment unfriendliness [11]. Therefore, special attention has been paid to the development of new red phosphors with high efficiency excited by near UV chips for the fabrication of WLEDs.

Recently, much attention has been paid on the orthophosphate phosphors due to their excellent properties such as large band gap, high chemical stability and high stability strong visible luminescence and also it required low sintering temperature for their synthesis. Luminescence of rare earth ions in phosphates has been widely studied in the past [12–15]. With the growing demand of a variety of light sources, the trivalent europium (Eu^{3+} ($4f^6$)) ions doped phosphors show great interest in the orange–red region because Eu^{3+} ions emits narrowband and almost monochromatic light and have long lifetime of the exited states. Therefore, it has been recognized as an efficient red emitter in WLEDs applications [16,17]. To the best of our knowledge, no investigations have been emphasized on the Eu^{3+} ions doped $K_4Ca(PO_4)_2$ host matrix. Due to the technological importance of

* Corresponding author at: Department of Future Studies, Sri Venkateswara University, Tirupati 517502, India. Tel.: +91 9440281769.
E-mail address: drdevaprasadraju@gmail.com (B. Deva Prasad Raju).

0022-2313/$ - see front matter © 2012 Elsevier B.V. All rights reserved.
http://dx.doi.org/10.1016/j.jlumin.2012.06.029

europium ion and the advantages the above research, the Eu^{3+} ions doped $K_4Ca(PO_4)_2$ phosphors are prepared. In addition to the detailed synthesis procedure of Eu^{3+} ions doped $K_4Ca(PO_4)_2$ host phosphors, the characterization results of XRD, FTIR, SEM, EDS, room temperature PL, decay curves and DSC analyses are discussed in this paper.

2. Material synthesis

The europium ions (Eu^{3+}) doped potassium calcium phosphate ($K_4Ca(PO_4)_2$) phosphors were prepared by the conventional high temperature solid state reaction method by sintering the samples at 1000 °C in air atmosphere. High purity raw materials K_2CO_3, $CaCO_3$, $NH_4H_2PO_4$ and Eu_2O_3 were obtained from commercial source (Merck, India). The nominal content of the activator ranges from 2 to 10 mol%. To obtain the homogeneous mixture, the stoichiometric ratios of these materials were ground thoroughly in an agate mortar for an hour. The resulting mixture was placed into a porcelain crucible and sintered at 1000 °C for 5 h in air atmosphere to get the final products. The obtained products were taken into different studies.

3. Characterization

The as-prepared phosphors were characterized by powder X-ray diffraction measurements on a Siemens X-ray diffractrometer AXS D 5005 with Cu Kα radiation (λ=1.5406 Å) at 40 kV and 20 mA and the 2θ ranges from 10° to 70°. To elucidate their composition and structure, the powders were also characterized by FTIR analysis on a Perkin Elmer spectrophotometer with KBr pellet technique in the range 4000–450 cm^{-1}. The morphology of the powder phosphor was inspected using a scanning electron microscopy (ZEISS EVO MA 15). The elemental composition of the as-prepared phosphor was quantified by energy dispersive spectroscopy (EDS) using an X-ray detector (THERMO EDS) attached to the SEM instrument. The thermal properties of $K_4Ca(PO_4)_2$ phosphor was carried out by DSC analysis using Mettler Toledo DSC 1 in the temperature range from 30 to 450 °C at a heating rate of 10 °C/min under the nitrogen atmosphere. The luminescent properties of these phosphors were performed by using Jobin Vyon Fluorolog-3 fluorescence spectrophotometer equipped with Xenon lamp as the excitation source. Decay curves of Eu^{3+}:$K_4Ca(PO_4)_2$ phosphors were also measured on this instrument. All the measurements were performed at room temperature.

4. Results and discussion

Fig. 1 shows the XRD patterns of Eu^{3+} (2, 6 and 10 mol%) doped $K_4Ca(PO_4)_2$ powder phosphors sintered at 1000 °C for 5 h. The XRD pattern of $K_4Ca(PO_4)_2$ crystal (JCPDS Card no.: 46-0629) is also shown in figure for comparison. It reveals that the XRD patterns of these samples are in good agreement with the JCPDS data. It also indicates that the Eu^{3+} ions have not caused any significant change after doped into the host lattice structure. All the observed peaks made for Eu^{3+}:$K_4Ca(PO_4)_2$ phosphor is found to be comparable with the XRD peaks of $K_4Ca(PO_4)_2$ reported by Rokbani and Kbir-Ariguib in 1990 [18]. It is considered that the trivalent europium (Eu^{3+}) ions substitute the possible cations (K^+, Ca^{2+} and P^{5+}) in $K_4Ca(PO_4)_2$ with the radii of K^+,Ca^{2+}, P^{5+} and Eu^{3+} for eight-coordinated sites (CN=8) are 0.151, 0.112, 0.017 and 0.1066 nm, respectively [19–21]. An acceptable percentage difference in ionic radii between doped and substituted ions must not exceed 30% [22]. The radius percentage difference between the doped and substituted ions can be calculated based

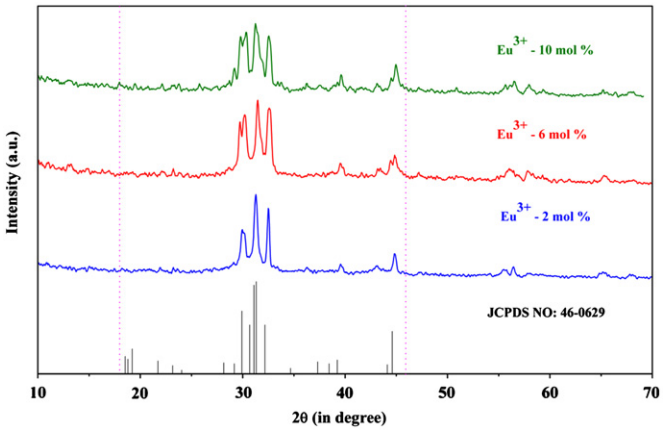

Fig.1. Powder XRD patterns of Eu^{3+} ions doped $K_4Ca(PO_4)_2$ phosphors sintered at 1000 °C.

on the following equation [23], $D_r=100\times[(R_m(CN)-R_d(CN))/R_m(CN)]$, where D_r is the radius percentage difference, CN is the coordination number, $R_m(CN)$ is the radius of the host cation, and $R_d(CN)$ is the radius of the doped ion. The estimated values of D_r between Eu^{3+} and K^+ and Eu^{3+} and Ca^{2+} on eight-coordinated sites are 29.40% and 4.82%, respectively, while the value of D_r between Eu^{3+} and P^{5+} is −527.05%. Based on the effective ionic radii (r) of cations with eight fold-coordinated (CN=8) sites, the rare earth ions are preferred to substitute the Ca^{2+} sites, because the effective ionic radii of Eu^{3+} (r=0.1066 nm) is close to that of Ca^{2+} (r=0.112 nm), while the K^+ sites are not occupied due to the effective ionic radii of eight-coordinated K^+ (r=0.151 nm) is too large compare to the rare earth ions. Therefore, we believed that the charge loss in Eu^{3+}:$K_4Ca(PO_4)_2$ is most probably compensated by Ca^{2+} vacancies (V_{Ca}), described by

$$3Ca^{2+}\rightarrow 2Eu^{3+}+V_{Ca}$$

Thus, we assumed that only one crystallographic site is occupied by Eu^{3+} in Eu^{3+}:$K_4Ca(PO_4)_2$. For analysis of the spectroscopic properties, the detailed crystal structure of the host material is important. Furthermore, much investigation on the crystal structure of $K_4Ca(PO_4)_2$ should be carried out in future for better understanding of the PL properties of this system.

Fig. 2 shows the obtained FTIR spectrum of $K_4Ca_{0.94}(PO_4)_2$:$Eu_{0.06}$ phosphor sintered at 1000 °C in air atmosphere. Generally, the characteristic bands of the orthophosphates are located in two regions of 1120–940 cm^{-1} and 650–540 cm^{-1} [24]. From the spectrum, it is clear that the main couple of absorption peaks are characteristics of the vibrations of $(PO_4)^{3-}$ groups: at 554 cm^{-1} for bending vibration and at 1053 cm^{-1} for stretching vibration. The strong absorption band in the region 2975–3500 cm^{-1} centered at 3230 cm^{-1} and the other sharp absorption peaks at 1403 and 1660 cm^{-1} are ascribed to the O–H content absorbed at the powder surface when the sample was in contact with the environment during the preparation process of measurement. A weak band at 2425 cm^{-1} might be due to the C–O vibration of CO_2 in the air. Moreover, the absence of characteristic bands of polyphosphates confirms that there is no polyphosphates in the sample, which is in good agreement with that of literature reported earlier [25,26].

The size distribution of the phosphor is significant for its application in LEDs, thus the SEM image of the $K_4Ca_{0.94}(PO_4)_2$:$Eu_{0.06}$ powder phosphor was examined and shown in Fig. 3. The morphology is formed by means of an aggregation process of high-active particles during calcinations and it possesses an irregular morphology. It is also clear from the microgram that

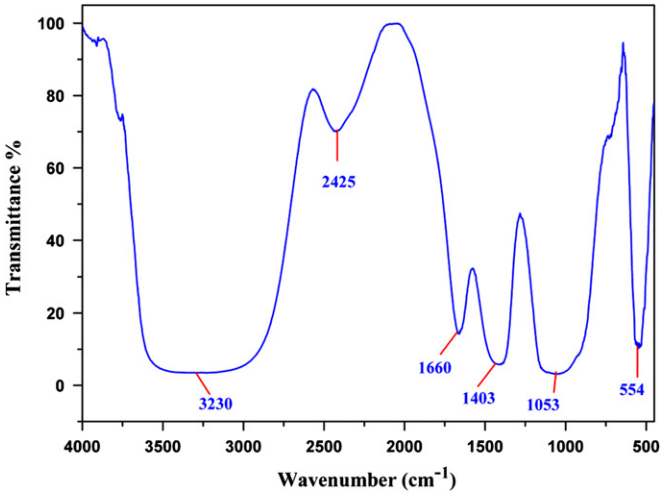

Fig. 2. FTIR spectrum of (6 mol%) Eu^{3+}:$K_4Ca(PO_4)_2$ powder phosphor.

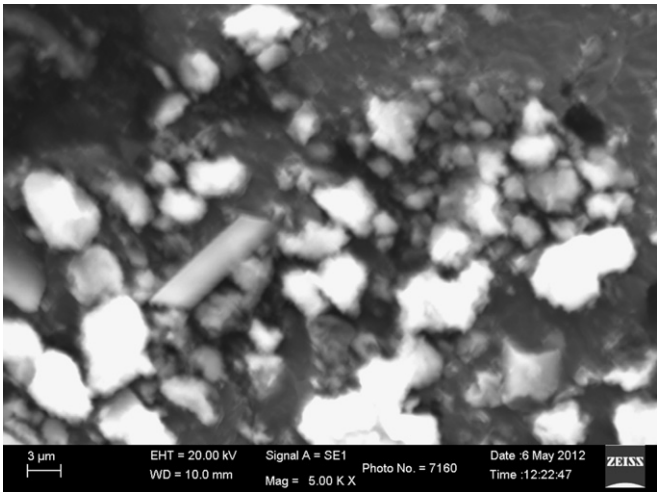

Fig. 3. SEM micrograph of (6 mol%) Eu^{3+}:$K_4Ca(PO_4)_2$ phosphor.

the average size of the particles may be in micrometer range, which is suitable for fabricating the solid-state lighting (SSL) devices. From the survey of literature, it is noticed that the crystalline powder that exhibits high luminescent intensities in addition with the micrometer dimension will find more applications [27,28]. In order to verify the presence of Eu in the doped $K_4Ca(PO_4)_2$ samples, the EDS analysis was performed. EDS profile of $K_4Ca_{0.94}(PO_4)_2$:$Eu_{0.06}$ phosphor is presented in Fig. 4 and it clearly revealed that the product is composed of K, Ca, P, O and Eu elements.

The recorded DSC profile is shown in Fig. 5. In the temperature region 30–450 °C, the DSC profile consists of two endothermic peaks: one is a broad endothermic peak located in the temperature range from 70 to 105 °C corresponds to the removal of free and adsorbed water [29] and the other a weak endothermic peak at 248 °C is due to the decomposition of NH_3 [30].

In order to estimate their potential application as the candidate phosphor for white light emitting diodes, the excitation and emission spectra of $K_4Ca(PO_4)_2$:Eu^{3+} phosphors were carried out. The recorded excitation spectrum of $K_4Ca_{0.98}(PO_4)_2$:$Eu_{0.02}$ powder phosphor sintered at 1000 °C is shown in Fig. 6. In the wavelength region 350–550 nm, several excitation peaks are observed and located at 362 nm ($^7F_0 \rightarrow {}^5D_4$), 382 nm ($^7F_0 \rightarrow {}^5L_7$), 394 nm ($^7F_0 \rightarrow {}^5L_6$), 415 nm ($^7F_0 \rightarrow {}^5D_3$), 465 nm ($^7F_0 \rightarrow {}^5D_2$) and 533 nm ($^7F_0 \rightarrow {}^5D_1$) which are assigned to 4f–4f transitions within the Eu^{3+} [31]. From the

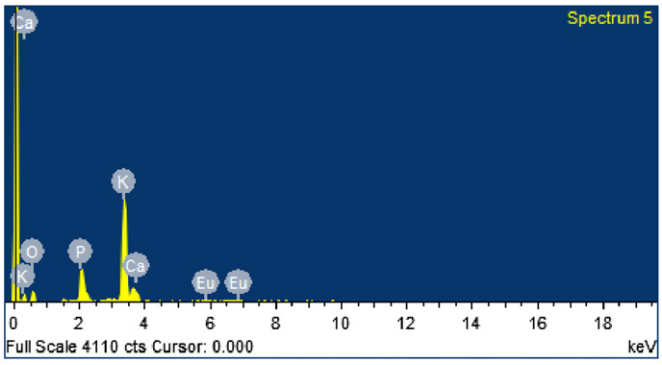

Fig. 4. EDS profile of (6 mol%) Eu^{3+}:$K_4Ca(PO_4)_2$ phosphor.

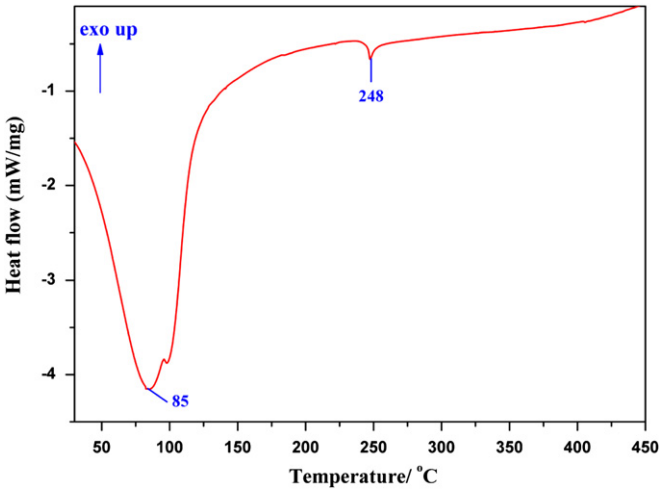

Fig. 5. DSC profile of (6 mol%) Eu^{3+}:$K_4Ca(PO_4)_2$ phosphor.

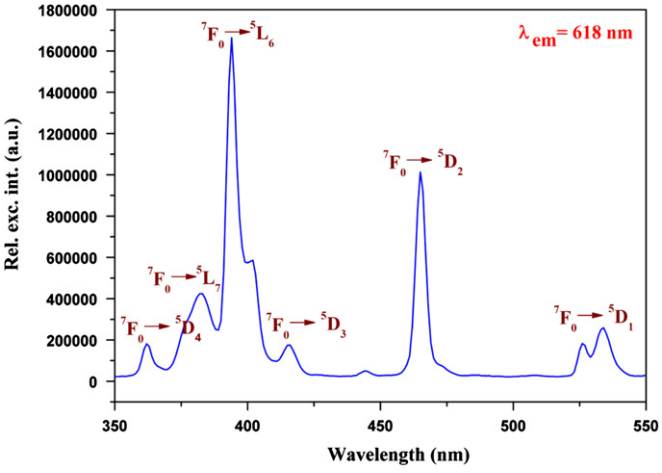

Fig. 6. Excitation spectrum of (2 mol%) Eu^{3+}:$K_4Ca(PO_4)_2$ phosphor.

spectrum, it was found that the intensity of f–f transition at 394 nm is high compared with the other transitions and has been chosen for the measurement of emission spectra of Eu^{3+}:$K_4Ca(PO_4)_2$ phosphors. The most intense peak obtained at 394 nm clearly suggests that these phosphors are effectively excited by near ultraviolet light emitting diodes (NUV-LEDs).

Fig. 7 shows the emission spectra of Eu^{3+} doped $K_4Ca(PO_4)_2$ phosphors. The emission band covers a region from 550 to 750 nm and it includes several typical emission sub-bands which

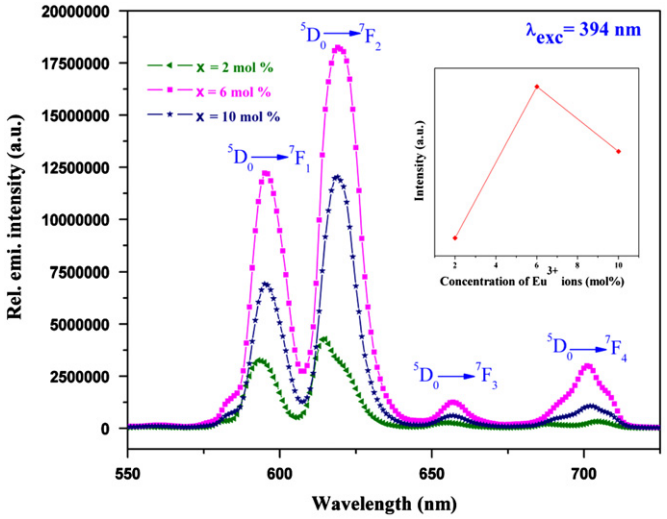

Fig. 7. Emission spectra of Eu_x^{3+}:$K_4Ca_{1-x}(PO_4)_2$ with an excitation wavelength of 394 nm. The inset shows the variation of PL intensity with rare earth ion (Eu^{3+}) concentration.

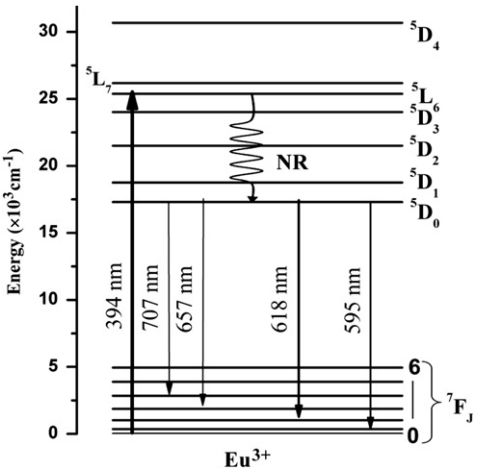

Fig. 8. The schematic energy level diagram of Eu^{3+} ions in $K_4Ca(PO_4)_2$ phosphors.

could be ascribed to the transition from $^5D_0 \rightarrow {}^7F_J$ ($J=1, 2, 3, 4$) are the characteristics of Eu^{3+} ions. The emission spectra contain the dominant red emission band at 618 nm is owing to the electric dipole transition of $^5D_0 \rightarrow {}^7F_2$, while the weak emission peak at 595 nm is due to the magnetic dipole transition of $^5D_0 \rightarrow {}^7F_1$. Other weak emission bands located at 657 and 707 nm could be ascribed to $^5D_0 \rightarrow {}^7F_3$ and $^5D_0 \rightarrow {}^7F_4$ transitions, respectively.

The luminescence originating from transitions between 4f levels is predominant due to electric dipole or magnetic dipole interactions [32]. It is well known that the intense red emission with the electric dipole transition $^5D_0 \rightarrow {}^7F_2$ is supersensitive to the symmetry of crystal field environment, while the orange–red emission with the magnetic dipole transition $^5D_0 \rightarrow {}^7F_1$ is insensitive to that. In order to detect the symmetry of the crystal field environment around Eu^{3+} ion, the intensity ratio (R) of transitions $^5D_0 \rightarrow {}^7F_2$ to $^5D_0 \rightarrow {}^7F_1$, $R=I_2/I_1$ was calculated [33]. The intensities I_2 and I_1 are defined as the area under their corresponding emission spectrum curves calculated by integrating from 610 to 630 nm and 585 to 609 nm, respectively. The symmetry local site without inversion center of the crystal field environment around Eu^{3+} leads to a higher value of ($R>1$), the opposite would lead to a lower value of R ($1>R>0$). The calculated R values for $K_4Ca_{1-x}(PO_4)_2$:Eu_x^{3+} ($x=2$, 6 and 10 mol%) phosphors are 1.42, 1.67 and 1.86, respectively, which indicated that Eu^{3+} occupies the sited with no inversion symmetry. From the spectra, it is clear that among the various characteristic transitions of Eu^{3+} ions, the hypersensitive electric dipole transition at 618 nm ($^5D_0 \rightarrow {}^7F_2$) was found to the dominant one. The energy level diagram of Eu^{3+} ions in $K_4Ca(PO_4)_2$:Eu^{3+} phosphor is depicted in Fig. 8.

In order to optimize the Eu^{3+} doping concentration to maximum the PL intensity, the Eu^{3+} doping concentration was varied according to $K_4Ca_{1-x}(PO_4)_2$:Eu_x^{3+} ($x=2$, 6 and 10 mol%). In Fig. 7, the inset shows the dependence of the PL intensity with rare earth ion (Eu^{3+}) concentration. From the emission spectra, it is also observed that by increasing the dopant (Eu^{3+}) concentration the PL intensity was also increased for 6 mol% and for 10 mol % the PL intensity was decreased due to concentration quenching effect. According to Dexter's theory, the decrease in the emission intensity occurs as a result of the non-radiative energy transfer between the Eu^{3+} ions, due to electric multipole–multipole interaction, which are distance dependent [34]. As the concentration of Eu^{3+} ions increases, the distance between these ions

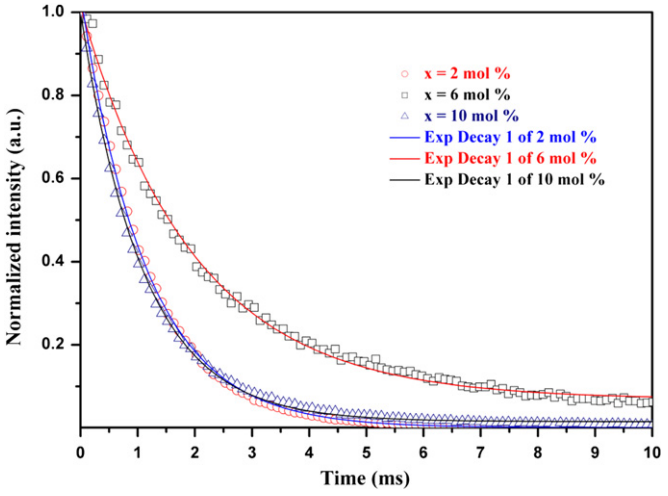

Fig. 9. Time decay patterns of 618 nm emission band for Eu_x^{3+}: $K_4Ca_{1-x}(PO_4)_2$ phosphors.

becomes smaller, with the result that the non-radiative pathway by energy transfer among the Eu^{3+} ions becomes preferential one [35]. Therefore, the optimum dopant concentration of Eu^{3+} ions for $K_4Ca_{1-x}(PO_4)_2$:Eu_x^{3+} ($x=2$, 6 and 10 mol%) is 6 mol%.

The luminescence decay curves of the 618 nm emission for $K_4Ca_{1-x}(PO_4)_2$:Eu_x^{3+} ($x=2$, 6 and 10 mol%) phosphors were recorded. Fig. 9 shows the decay curves for $^5D_0 \rightarrow {}^7F_2$ emission for these samples when excited at 394 nm. All these curves can be well fitted into single-exponential decay equation, revealing that the presence of the Eu^{3+} environment is unique in accordance with the crystal structure. Additionally, no wavelength shift or peak for a new site has been observed for various concentrations. This implies that only one local Eu^{3+} environment exists, because different centers will have different excitation and emission spectra, which is in consistent with the XRD results [36]. However, the predominant single exponential behavior indicating the homogeneous of doped ions inside the host matrix. In the past, Barthon et al. [37] had reported that the decay time would decrease if there were a large number of de-excited centers that rapidly transited to ground state. On the basis of equation, $I=I_0 \exp(-t/\tau)$, the lifetime values of $K_4Ca_{1-x}(PO_4)_2$:Eu_x^{3+} ($x=2$, 6 and 10 mol%) were determined to be 1.1528, 1.982 and 1.094 ms, respectively. As the Eu^{3+} dopant concentration increases, the concentration quenching effect occurs, and it will degenerate the emission intensity and the decay time.

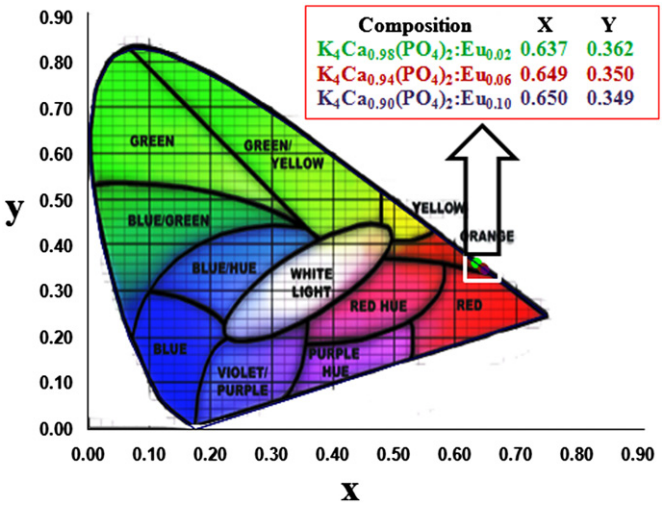

Fig. 10. CIE color coordinates of Eu^{3+}: $K_4Ca(PO_4)_2$ phosphors.

To evaluate the material performance on color luminescent emission, the Commission International de l'Eclairage (CIE) chromaticity coordinates *X, Y* were obtained for the prepared samples. The CIE chromaticity coordinates of the light emission from these Eu^{3+} doped $K_4Ca(PO_4)_2$ phosphors excited at 394 nm are depicted in Fig. 10. It indicates that the color of the phosphors with different Eu^{3+} ion contents lies in the orange-reddish region for prepared phosphors and the CIE values varying from (0.637, 0.362) to (0.650, 0.349). The coordinate of *X* increases with the increase of Eu^{3+} ion contents, whereas the value of *Y* decreases with the increase of Eu^{3+} ion. However, the largest values of *X* and *Y* are 0.650 and 0.362 corresponds to 10 and 2 mol% of Eu^{3+} ions, respectively. This demonstrates that the $K_4Ca(PO_4)_2:Eu^{3+}$ phosphors are potential materials for the fabrication of NUV WLEDs.

5. Conclusions

In conclusion, we have successfully synthesized novel and red luminescent $K_4Ca_{1-x}(PO_4)_2:Eu_x^{3+}$ ($x=2$, 6 and 10 mol%) phosphors by the conventional solid state reaction technique at 1000 °C for 5 h in air atmosphere and their luminescence have been studied and discussed for the first time. FTIR spectrum evidences the existence of $(PO_4)^{3-}$ groups in these phosphors. SEM micrograph indicated that the particles are found to be in micrometer size, which is suitable for the fabrication of the SSL devices. In addition, the elemental composition is verified with EDS analysis and the DSC analysis has been carried out to study the thermal properties. Most importantly, the Eu^{3+} doped $K_4Ca(PO_4)_2$ samples exhibit strong red emission at 618 nm ($^5D_0 \rightarrow {}^7F_2$) under the near UV excitation wavelength of 394 nm ($^7F_0 \rightarrow {}^5L_6$). The $K_4Ca(PO_4)_2:Eu^{3+}$ phosphor has the strongest emission intensity, when the doping concentration of Eu^{3+} is 6 mol%. Based on these obtained results, we propose that the newly developed $K_4Ca(PO_4)_2:Eu^{3+}$ phosphors are a promising candidate as a red component for the fabrication of near UV based white LEDs.

Acknowledgment

The authors are highly grateful to Prof. C.K. Jayasankar, Prof. P. Sreedhar Reddy and Prof. O.Md. Hussain, Department of Physics, Sri Venkateswara University, Tirupati, for permitting us to utilize their laboratory facilities. The authors are sincerely thankful to XRD facility extended by Dr. C. Shivakumara, Senior Scientific Officer, Solid State and Structural Chemistry Unit, Indian Institute of Science (IISc), Bangalore. The authors also acknowledge Sophisticated Analytical Instrumentation Facility (SAIF), IIT, Chennai and Spectroscopy/Analytical Test Facility (SATF), IISc, Bangalore for extending the instrumental facilities.

References

[1] A.K. Parchur, R.S. Nigthoujan, S.B. Rai, G.S. Okram, R.A. Singh, M. Tyagi, S.C. Gadkari, R. Tewari, R.K. Vasta, Dalton Trans. 40 (2011) 7595.
[2] A.S. Barker Jr, Phys. Rev. 135 (1964) A742.
[3] V.M. Longom, A.T.D. Figueiredo, A.B. Campos, J.W.M. Espinosa, A.C. Hernandes, C.A. Taft, J.R. Sambrano, J.A. Varela, E. Longo, J. Phys. Chem. A 112 (2008) 8920.
[4] X. Liu, L. Yan, J. Lin, J. Phys. Chem. C 113 (2009) 8478.
[5] S. Enhai, Z. Weiren, Z. Gouxiong, D. Xihua, Y. Chunyu, Z. Minkang, J. Rare Earths 29 (2011) 440.
[6] S. Nakamura, G. Fasol, The Blue Laser Diode: GaN Based Light Emitting and Lasers, Springer, Berlin, 1997.
[7] T.W. Kuo, W.R. Lin, T.M. Chen, Opt. Express 18 (2010) 1888.
[8] W.R. Lin, Y.C. Chin, Y.T. Yen, S.M. Jang, T.M. Chen, J. Electrochem. Soc. 156 (2009) J165.
[9] S. Sailaja, S.J. Dhoble, B.S. Reddy, J. Mol. Struct. 1003 (2011) 115.
[10] M. Zhang, J. Wang, Q.H. Zhang, W.J. Ding, Q. Su, Mater. Res. Bull. 42 (2007) 33.
[11] Q. Zhang, J. Wang, R. Yu, M. Zhang, Q. Su, Electrochem. Solid-State Lett. 11 (2008) H335.
[12] X. Wang, F. Du, D. Wei, Y. Huang, H.J. Seo, Sensors Actuators B 158 (2011) 171.
[13] T.J. Xie, N. Hirosaki, Sci. Technol. Adv. Mater. 8 (2007) 588.
[14] L. Shi, Y. Huang, H.J. Seo, J. Phys. Chem. A 114 (2010) 6927.
[15] C. Qin, Y. Huang, L. Shi, G. Chen, X. Qiao, H.J. Seo, J. Phys. D: Appl. Phys. 42 (2009) 185105.
[16] S. Sailaja, S.J. Dhoble, N. Brahme, B.S. Reddy, J. Mater. Sci. 46 (2011) 7793.
[17] A.A. Setlur, J.J. Shiang, U. Happek, Appl. Phys. Lett. 92 (2008) 081104.
[18] R. Rokbani, N. Kbir-Ariguib, Thermochim. Acta 159 (1990) 201.
[19] Li Wu, Yi Zhang, Mingyuan Gui, Pengzhi Lu, Lixia Zhao, Shu Tian, Yongfa Kong, Jingjun Xu, J. Mater. Chem. 22 (2012) 6463.
[20] B.K. Grandhe, V.R. Bandi, K. Jang, S.S. Kim, D.S. Shin, Y.I. Lee, J.M. Lim, T. Song, J. Alloys Compd. 509 (2011) 7937.
[21] W. Gu, M. Shen, X. Chang, Y. Wang, J. Wang, J. Alloys Compd. 441 (2007) 311.
[22] M. Penga, G. Hong, J. Lumin. 127 (2007) 735.
[23] S. Yao, Y. Li, L. Xue, Y. Yan, Int. J. Appl. Ceram. Technol. 8 (2011) 701.
[24] B. Yue, J. Gu, G. Yin, Z. Huang, X. Liao, Y. Yao, Y. Kang, P. You, Curr. Appl. Phys. 10 (2010) 1216.
[25] Y. Huang, X. Wang, H.S. Lee, E. Cho, K. Jang, Y. Tao, J. Phys. D: Appl. Phys. 40 (2007) 7821.
[26] R.A. Nyquist, R.O. Kagel, Infrared Spectra of Inorganic Compounds (3800–45 cm^{-1}), Academic Press, NY, 1992 (p. 232).
[27] B. Yan, C. Wang, Solid State Sci. 10 (2008) 82.
[28] V.R. Bandi, B.K. Grandhe, M. Jayasimhadri, K. Jang, H.S. Lee, S.S. Yi, J.H. Jeong, J. Cryst. Growth 326 (2011) 120.
[29] S. Dong, X. Cui, Z. Fu, S. Zhou, S. Zhang, Z. Dai, Mater. Res. Bull. 47 (2012) 212.
[30] L. Zhang, Z. Lu, H. Yang, P. Han, N. Xu, Q. Zhang, J. Alloys Compd. 512 (2012) 5.
[31] G. Ping, X. Wang, Y. Wu, L. Qin, K. She, Opt. Mater. 34 (2012) 748.
[32] G.M. Cai, F. Zheng, D.Q. Yi, Z.P. Jin, X.L. Chen, J. Lumin. 130 (2010) 910.
[33] L.L. Su, G. Li, G.S. Li, Chem. Mater. 20 (2008) 6060.
[34] D.L. Dexter, J. Chem. Phys. 21 (1953) 836.
[35] D.K. Yim, I.S. Cho, C.W. Lee, J.H. Noh, H.S. Roh, K.S. Hong, Opt. Mater. 33 (2011) 1036.
[36] Y.C. Li, Y.H. Chang, Y.F. Lin, Y.S. Chang, Y.J. Lin, J. Alloys Compd. 439 (2007) 367.
[37] C. Barthou, J. Benoit, J. Benalloul, A. Morell, J. Electrochem. Soc. 141 (1994) 524.